Available online at www.sciencedirect.com
ScienceDirect
Journal of Power Sources 163 (2007) 1053–1058
JOURNAL OF POWER SOURCES
www.elsevier.com/locate/jpowsour

Short communication

Synthesis and characterization of submicron-sized $LiNi_{1/3}Co_{1/3}Mn_{1/3}O_2$ by a simple self-propagating solid-state metathesis method

Yu-Shi He [a], Zi-Feng Ma [a,*], Xiao-Zhen Liao [a], Yi Jiang [b]

[a] *Department of Chemical Engineering, Shanghai Jiao Tong University, Shanghai 200240, PR China*
[b] *Instrumental Analysis Center, Shanghai Jiao Tong University, Shanghai 200030, PR China*

Received 28 July 2006; received in revised form 21 September 2006; accepted 27 September 2006
Available online 13 November 2006

Abstract

Submicron-sized $LiNi_{1/3}Co_{1/3}Mn_{1/3}O_2$ cathode materials were synthesized using a simple self-propagating solid-state metathesis method with the help of ball milling and the following calcination. A mixture of $Li(ac)\cdot 2H_2O$, $Ni(ac)_2\cdot 4H_2O$, $Co(ac)_2\cdot 4H_2O$, $Mn(ac)_2\cdot 4H_2O$ (ac = acetate) and excess $H_2C_2O_4\cdot 2H_2O$ was used as starting material without any solvent. XRD analyses indicate that the $LiNi_{1/3}Co_{1/3}Mn_{1/3}O_2$ materials were formed with typical hexagonal structure. The FESEM images show that the primary particle size of the $LiNi_{1/3}Co_{1/3}Mn_{1/3}O_2$ materials gradually increases from about 100 nm at 700 °C to 200–500 nm at 950 °C with increasing calcination temperature. Among the synthesized materials, the $LiNi_{1/3}Co_{1/3}Mn_{1/3}O_2$ material calcined at 900 °C exhibits excellent electrochemical performance. The steady discharge capacities of the material cycled at 1 C (160 mA g^{-1}) rate are at about 140 mAh g^{-1} after 100 cycles in the voltage range 3–4.5 V (versus Li^+/Li) and the capacity retention is about 87% at the 350th cycle.

Keywords: Lithium-ion battery; Self-propagating solid-state metathesis; FESEM; Submicron-sized; $LiNi_{1/3}Co_{1/3}Mn_{1/3}O_2$

1. Introduction

Rechargeable lithium-ion batteries have been widely investigated in the field of portable power sources owing to their high power density and long operational life. $LiCoO_2$, $LiNi_{0.8}Co_{0.2}O_2$ and $LiMn_2O_4$ are currently used as cathode materials in commercial lithium-ion batteries [1–4]. Cobalt-based and nickel-based layered compounds are relative expensive and toxic. $LiMn_2O_4$ spinels are attractive, with low cost and low toxicity; however, they have low specific capacity and suffer from serious capacity fading during cycling, especially under high temperature [5,6].

Recently, layered $LiNi_{1/3}Co_{1/3}Mn_{1/3}O_2$ compound developed by Ohzuku and Makimura [7] has been considered as an attractive candidate of next-generation cathode materials to replace $LiCoO_2$ for rechargeable lithium-ion batteries due to its large capacity and stable structure. $LiNi_{1/3}Co_{1/3}Mn_{1/3}O_2$ cathode material has been traditionally synthesized by hydroxide co-precipitation [8–12]. The co-precipitation method could give phase-pure oxide products and high tap-density spherical powders with uniform distribution. But this synthesis method must control the pH value of the solution at a range and precipitated $Mn(OH)_2$ is easily oxidized to MnOOH or MnO_2 without inert gas protection in preparing precursor [13,14]. Furthermore, filtering, washing and precalcination procedures are also required. Thus, it is very difficult to reproductively prepare the same sample. So, it is necessary to develop a new synthesis route for $LiNi_{1/3}Co_{1/3}Mn_{1/3}O_2$ compound. Caballero et al. [15] developed a simple solvent-free method for preparing nanometric cathode materials, including $LiMn_2O_4$, $LiNi_{0.5}Mn_{1.5}O_4$, $LiCoO_2$ and $LiCo_{0.5}Ni_{0.5}O_2$. The method is based on the preparation of oxalate precursor by one-step solid-state metathesis reactions of various hydrated salts in the presence of hydrated oxalic acid [16,17]. In the solid-state metathesis procedure, no solvent is added which could effectively avoid the occurrence of concentration gradient in precursor and simplify the preparation process. A disadvantage of the method is, however, the limitation of the raw salt materials. Some of them are relatively expensive. In this paper, the submicron-sized $LiMn_{1/3}Ni_{1/3}Co_{1/3}O_2$ cathode material was prepared by using the self-propagating

* Corresponding author. Tel.: +86 21 54742894; fax: +86 21 54741297.
E-mail address: zfma@sjtu.edu.cn (Z.-F. Ma).

0378-7753/$ – see front matter © 2006 Elsevier B.V. All rights reserved.
doi:10.1016/j.jpowsour.2006.09.061

solid-state metathesis method, the structure and electrochemical properties of the prepared materials were systematically investigated. This paper firstly reveals the structure of the intermediary products resulting from the self-propagating solid-state metathesis reaction and optimum conditions for synthesis of $LiNi_{1/3}Co_{1/3}Mn_{1/3}O_2$ via the method.

2. Experimental

Submicron-sized $LiNi_{1/3}Co_{1/3}Mn_{1/3}O_2$ powders were prepared by thermal decomposition of mixed oxalates formed by grinding acetate salts with oxalic acid. $Li(ac)\cdot 2H_2O$, $Ni(ac)_2\cdot 4H_2O$, $Co(ac)_2\cdot 4H_2O$ and $Mn(ac)_2\cdot 4H_2O$ (ac = acetate) were mixed in appropriate proportions with excess $H_2C_2O_4\cdot 2H_2O$ without adding any solvent. The mixtures were ballmilled for 3 h in a planetary mill (Pulueriset 6) with agate vessels. The obtained pink colored mixture was air-dried at 120 °C for 12 h and then directly calcined at various temperatures at a heating rate of 4 °C min^{-1} for 20 h in atmosphere to obtain final $LiNi_{1/3}Co_{1/3}Mn_{1/3}O_2$ products without any precalcination procedure.

Thermogravimetric analysis (TG) for the ballmilled mixture was carried out using a Perkin-Elmer model 7 instrument to determine approximate calcining temperature and procedure. The mixture sample was heated at 10 °C min^{-1} from room temperature to 800 °C in a flowing air atmosphere. The XRD patterns were collected by a Philips 3100E diffractometer using Cu Kα radiation (λ = 1.5406 Å). The samples were scanned for 2θ values in the range from 10° to 80°. The particle morphology of powders after calcination was observed using a field emission scanning electron microscope (FESEM, JSM-7401F, JEOL, Japan) at an accelerating voltage of 15 kV. $LiNi_{1/3}Co_{1/3}Mn_{1/3}O_2$ working electrodes were prepared by slurrying 75% $LiNi_{1/3}Co_{1/3}Mn_{1/3}O_2$ powder, 15% acetylene black and 10% polyvinylidene fluoride (PVDF) in a volatile solvent, and then casting the mixture onto an aluminum foil. After vacuum drying at 120 °C for about 8 h, the electrode disks (Ø 14 mm) were punched and weighed. The active material loaded on the electrode disks was about 9.1 mg cm^{-2}. The $LiNi_{1/3}Co_{1/3}Mn_{1/3}O_2$ working electrodes were incorporated into cells with a lithium foil counter electrode, a UP3025 separator (provided by UBE Industries, Ltd., Japan), and 1 M $LiPF_6$ electrolyte in a dimethyl carbonate (DMC) and ethylene carbonate (EC) mixed solvent of 1:1 (LP30 from EM Industries, Inc.). The cells were assembled in an argon-filled glove box. Cycling performance of $LiNi_{1/3}Co_{1/3}Mn_{1/3}O_2$ cathode material was evaluated using a battery test system (BT-8 model, Arbin Instruments Inc.) under a constant current condition. Cyclic voltammetry (CV) was performed using a Solartron SI1287 electrochemical interface controlled by Corrware at a scanning rate 0.1 mV s^{-1}. All tests were performed at room temperature.

3. Results and discussion

Fig. 1 shows the TG-DTG curve for the ballmilled mixture. Two distinct weight loss steps in the temperature range of

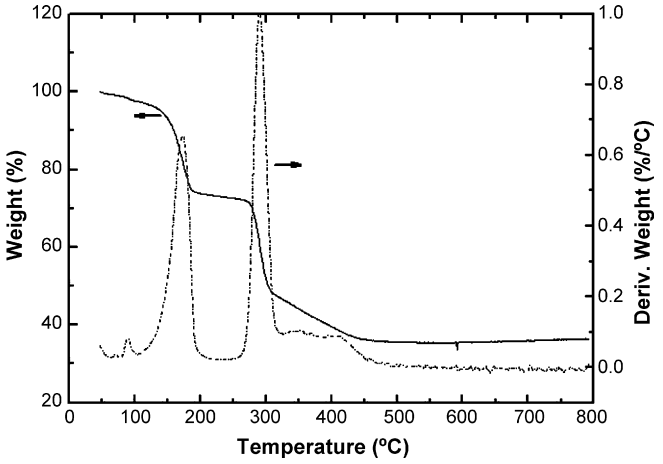

Fig. 1. TG-DTG curve for the ballmilled product.

100–220 and 220–320 °C were observed, and it can be attributed to the lost crystal water and the decomposition of the oxalate, respectively [15,18]. The ball milling would cause a metathesis reaction between the acetate salts and $H_2C_2O_4\cdot 2H_2O$. It is apparent that the crystalline (or coordinated) water in hydrated metal salts plays an important role in the solvent-free solid-state reactions. It can be seen, a third step showing a slow weight loss from 320 to 550 °C. The weight loss is almost zero above 550 °C, which indicates that $LiNi_{1/3}Co_{1/3}Mn_{1/3}O_2$ material will completely form above this temperature.

The XRD patterns of the ballmilled mixture and the standard $CoC_2O_4\cdot 2H_2O$ (JCPDS 25-0251) are given in Fig. 2. As shown in Fig. 2, the diffraction pattern of the mixture well agree with the standard monoclinic $CoC_2O_4\cdot 2H_2O$. The broad integrated diffraction lines could be ascribed to the mixture of transition metal oxalates such us $CoC_2O_4\cdot 2H_2O$, $NiC_2O_4\cdot 2H_2O$ and $MnC_2O_4\cdot 2H_2O$. The $Li_2C_2O_4$ obtained by metathesis reaction is also indexed in Fig. 2. Therefore, the ballmilled mixture should be the mixture of transition metal oxalates and $Li_2C_2O_4$.

Fig. 3 shows the XRD patterns of the $LiNi_{1/3}Co_{1/3}Mn_{1/3}O_2$ cathode materials obtained by heating the ballmilled mixtures at

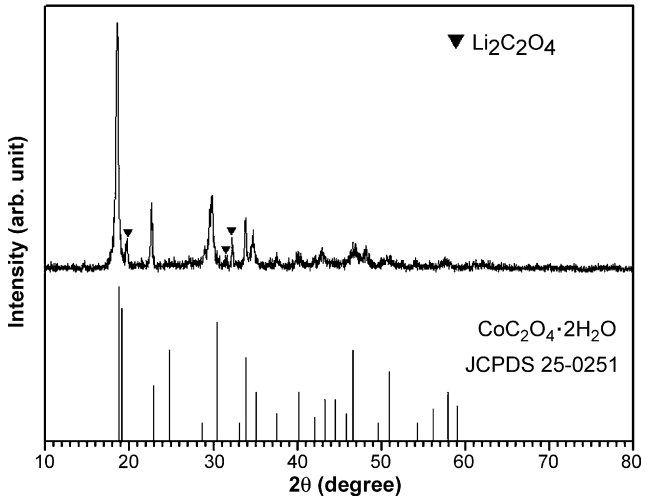

Fig. 2. X-ray diffraction pattern for the ballmilled product.

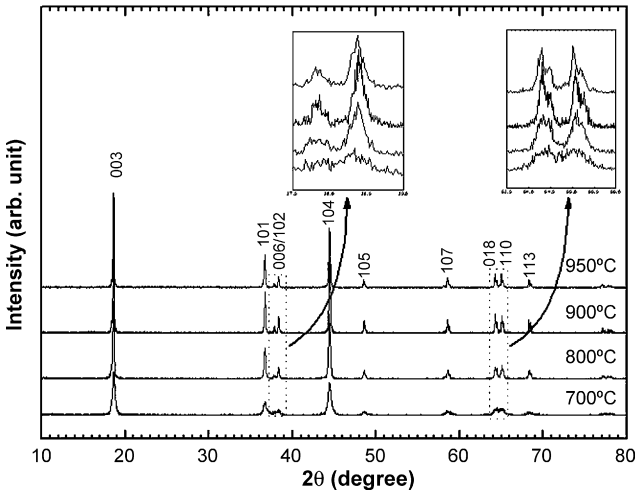

Fig. 3. X-ray diffraction patterns of $LiNi_{1/3}Co_{1/3}Mn_{1/3}O_2$ samples calcined at different temperatures.

different temperature from 700 to 950 °C. The XRD patterns of all materials could be indexed by a hexagonal α-$NaFeO_2$ structure (space group: 166, $R\bar{3}m$) and no obvious impurity phase could be observed in the XRD patterns. In XRD patterns, the integrated intensity ratio of (0 0 3)/(1 0 4) peaks and the splitting of (0 0 6)/(1 0 2) peaks and (0 1 8)/(1 1 0) peaks are regarded as the indications of characteristic of layered structure materials [19,20]. It was reported that the undesirable cation mixing would take place if the integrated intensity ratio of (0 0 3)/(1 0 4) peaks is less than 1.2. According to the XRD pattern illustrated in Fig. 3, the (0 0 6) and (1 0 2) peaks and (0 1 8) and (1 1 0) peaks are clearly split when the heating temperature is above 800 °C. The lattice parameters calculated by the least-square method using 10 diffraction lines and the integrated intensity ratio of (0 0 3)/(1 0 4) peaks are listed in Table 1. The unit cell volume increases from 101.31 $Å^3$ at 800 °C to 101.46 $Å^3$ at 950 °C with increasing sintered temperature. Based on the above results, it is clear that $LiNi_{1/3}Co_{1/3}Mn_{1/3}O_2$ material calcined at 900 °C has minimal cation mixing and may result in good electrochemical performance.

The field-emission SEM (FESEM) images of $LiNi_{1/3}Co_{1/3}Mn_{1/3}O_2$ materials calcined at different temperatures for 20 h are shown in Fig. 4. With increasing calcination temperature, the primary particle size gradually increases from about 100 nm at 700 °C to 200–500 nm at 950 °C, and the edges of the particles become much sharper. It could be noticed that $LiNi_{1/3}Co_{1/3}Mn_{1/3}O_2$ samples calcined at 700 and 800 °C exhibit relative uniform particle size, as shown in Fig. 4a and b, while $LiNi_{1/3}Co_{1/3}Mn_{1/3}O_2$ materials calcined at 900 and 950 °C consist of some small primary particles and larger secondary ones. It indicates that raising the calcined temperature not only increase particle size, but also affect the uniformity of the materials.

Fig. 5 shows the typical initial charge–discharge curves of $LiNi_{1/3}Co_{1/3}Mn_{1/3}O_2$ materials heat treated at various calcined temperatures. The cycling performance for the prepared $LiNi_{1/3}Co_{1/3}Mn_{1/3}O_2$ materials is illustrated in Fig. 6. The cell was cycled between 3 and 4.3 V at a low current density of 16 mA g^{-1} (0.1 C). As shown in Fig. 5, the prepared $LiNi_{1/3}Co_{1/3}Mn_{1/3}O_2$ materials display smooth charge/discharge curves without any plateaus. This indicates that no spinel-related phases are formed during charging and discharging. The initial charge–discharge curves of the samples calcined at 700 and 800 °C are quite similar. The first discharge capacities of $LiNi_{1/3}Co_{1/3}Mn_{1/3}O_2$ materials calcined at 700, 800, 900 and 950 °C are 145.7, 146.2, 162.4 and 159.4 mAh g^{-1}, respectively. The initial irreversible capacities are about 15–25 mAh g^{-1}. This may be attributed to the formation of a SEI film on the surface of the electrode and insufficient soaking of the electrode material during the first cycle [21]. According to Fig. 6, the $LiNi_{1/3}Co_{1/3}Mn_{1/3}O_2$ material calcined at 900 °C achieves high discharge capacity with a slight capacity fade. The retention value of capacity is 93.7% after 20 cycles. It corresponds with the results observed by above XRD patterns. The cycling stability of the sample calcined at 950 °C is not very satisfied and the discharge capacity of the sample retains only 81.3% after 20 cycles. It may be attributed to the large primary particle size that makes the intercalation/deintercalation of Li ions difficult in the cycling process [22]. In the following content, the electrochemical performance of the sample calcined at 900 °C will be discussed in detail.

Fig. 7 shows the discharge capacity as a function of cycle number for $LiNi_{1/3}Co_{1/3}Mn_{1/3}O_2$ material calcined at 900 °C with various charge cutoff voltages at a current density of 16 mA g^{-1} (0.1 C). When the upper limit voltage is raised to 4.4, 4.5 and 4.6 V, the discharge capacities of the cell are 164.1, 174.9 and 186.3 mAh g^{-1}, respectively. The cell in different voltage ranges presents good cycleability.

Fig. 8 shows the cycling performance of $LiNi_{1/3}Co_{1/3}Mn_{1/3}O_2$ cathode at different rates. The cells were cycled at the 0.1 C (16 mA g^{-1}) rate for the initial five cycles before each rate test. Then the cells were charged/discharged using 160 mA g^{-1} (1 C, Fig. 8a) and 320 mA g^{-1} (2 C, Fig. 8b) constant current between 3 and 4.5 V, respectively. The constant voltage (4.5 V) charge was applied to each cell until the current was decreased

Table 1
Structural parameters of $LiNi_{1/3}Co_{1/3}Mn_{1/3}O_2$ samples calcined at different temperatures

Samples	Heating temperatures (°C)	a (Å)	c (Å)	Volume ($Å^3$)	c/a	$I_{(003)}/I_{(104)}$[a]
1	800	2.8636	14.2646	101.31	4.9812	1.09
2	900	2.8646	14.2612	101.35	4.9783	1.26
3	950	2.8656	14.2662	101.46	4.9784	1.17

[a] $I_{(003)}/I_{(104)}$ is the ratio of the integrated intensities of the (0 0 3) and (1 0 4) peaks.

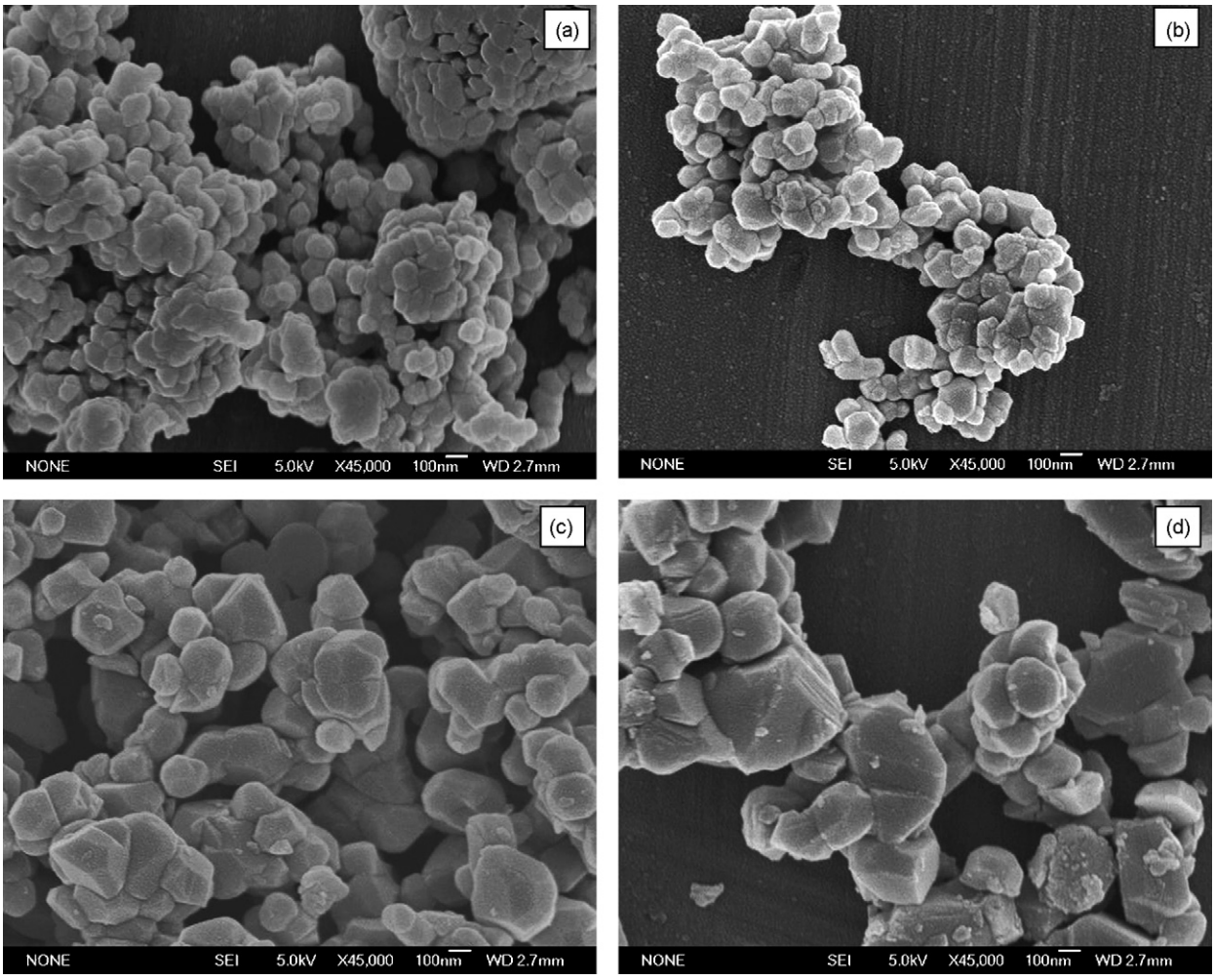

Fig. 4. FESEM images of $LiNi_{1/3}Co_{1/3}Mn_{1/3}O_2$ samples calcined at (a) 700 °C, (b) 800 °C, (c) 900 °C and (d) 950 °C for 20 h.

to 1/10th of its initial value during charging process. As shown in Fig. 8a, the steady discharge capacities of the cell cycled at 1 C rate could be still achieved at about 140 mAh g^{-1} after 100 cycles and the capacity retention was about 87% at the 350th cycle. Furthermore, the discharge capacity of the cell cycled at 2 C rate retained 88.5% of its original value after 60 cycles in Fig. 8b. The excellent rapid charge–discharge cyclic performance of $LiNiCo_{1/3}Mn_{1/3}O_2$ cathode could be

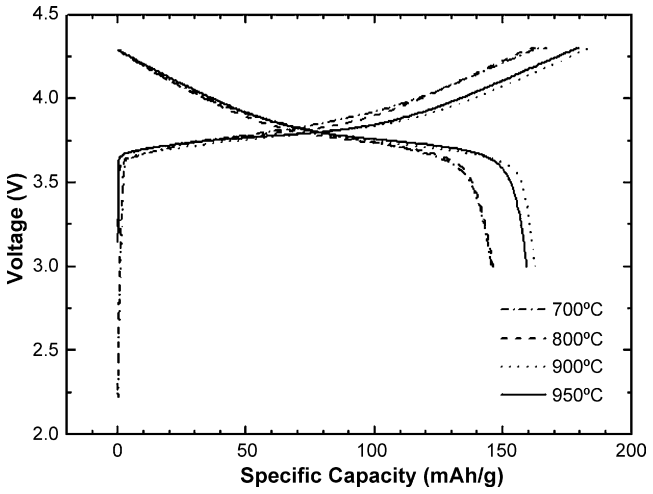

Fig. 5. Initial charge–discharge curves of $LiNi_{1/3}Co_{1/3}Mn_{1/3}O_2$ samples calcined at various temperatures in the voltage range 3–4.3 V.

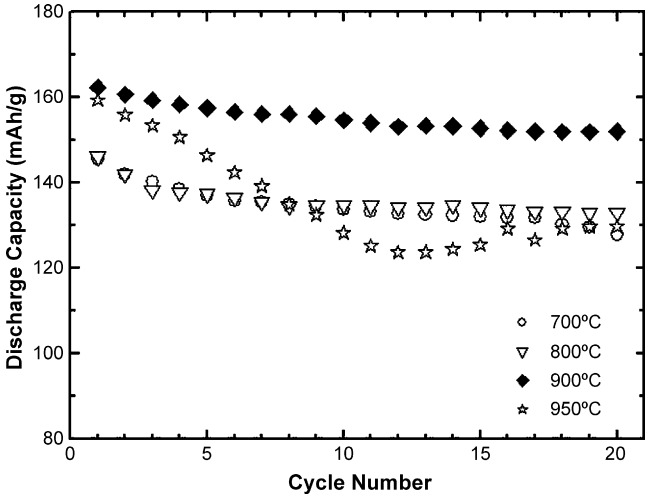

Fig. 6. Cycling performance of $LiNi_{1/3}Co_{1/3}Mn_{1/3}O_2$ samples calcined at various temperatures in the voltage range 3–4.3 V.

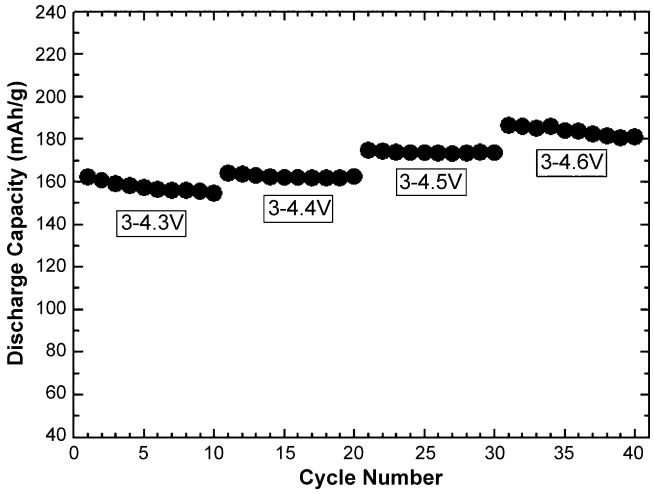

Fig. 7. Discharge capacity as a function of cycle number for $LiNi_{1/3}Co_{1/3}Mn_{1/3}O_2$ sample calcined at 900 °C with various charge cutoff voltages at a current density of 16 mA g^{-1} (0.1 C).

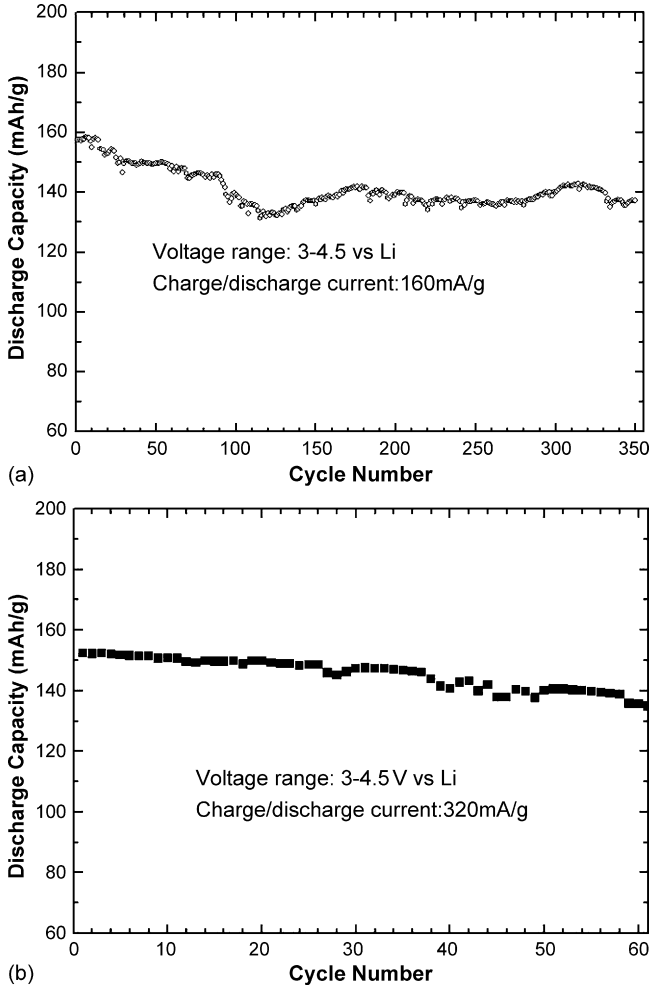

Fig. 8. Cycling performance of $LiNi_{1/3}Co_{1/3}Mn_{1/3}O_2$ cathode at the different discharge current density of (a) 160 mA g^{-1} (1 C) and (b) 320 mA g^{-1} (2 C).

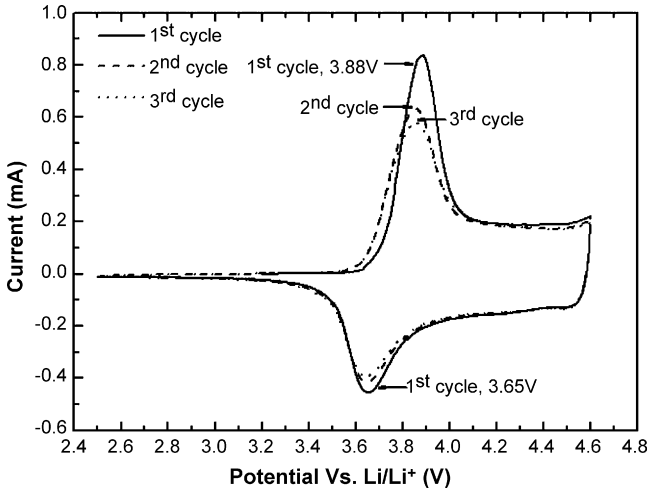

Fig. 9. CVs of $LiNi_{1/3}Co_{1/3}Mn_{1/3}O_2$ cathode material in an electrolyte of 1 M $LiPF_6$ in a 1:1 EC:DMC solvent at a sweep rate of 0.1 mV s^{-1}.

attributed to its special microstructure developed in the self-propagating solid-state metathesis method using the ballmilling procedure.

Fig. 9 shows a typical CV of $LiNiCo_{1/3}Mn_{1/3}O_2$ cathode material between 2.5 and 4.6 V. It is noted that no anodic peak at around 4.5 V corresponding to irreversible capacity is observed in the first cycle [23,24]. The appearance of only one redox couple between 2.5 and 4.6 V suggests that structural transition from hexagonal to monoclinic structure do not exist [25]. The reproducibility of the second and third cycle peaks represents a good reversibility of the $LiNiCo_{1/3}Mn_{1/3}O_2$ electrode. The potential separation of the second cycle between the anode and cathode peak is less than for the first cycle. Furthermore, no peak around 3 V means that Mn^{3+} ions are not present [26,27].

4. Conclusion

The layered submicron-sized $LiNi_{1/3}Co_{1/3}Mn_{1/3}O_2$ cathode materials were successfully synthesized by a simple self-propagating solid-state metathesis method. A mixture of $Li(ac)\cdot 2H_2O$, $Ni(ac)_2\cdot 4H_2O$, $Co(ac)_2\cdot 4H_2O$, $Mn(ac)_2\cdot 4H_2O$ (ac = acetate) and excess $H_2C_2O_4\cdot 2H_2O$ was used as starting material without any solvent. The starting mixture was ball milled for 3 h to form an oxalate mixture as a result of the metathesis reaction between the acetate salts and $H_2C_2O_4\cdot 2H_2O$. The product of ball milling was then calcined under different temperatures (700, 800, 900 and 950 °C) to obtain the final submicron-sized $LiNi_{1/3}Co_{1/3}Mn_{1/3}O_2$ powders. When the heating temperature is above 800 °C, the clear peak splits of the (0 0 6)/(1 0 2) peaks and (0 1 8)/(1 1 0) peaks in XRD patterns of the $LiNi_{1/3}Co_{1/3}Mn_{1/3}O_2$ materials are shown. The $LiNi_{1/3}Co_{1/3}Mn_{1/3}O_2$ material calcined at 900 °C shows a high electrochemical capacity and good cycleability at different rates. These results indicate that the self-propagating solid-state metathesis method is a simple but efficient synthesis route for preparing high-performance $LiNi_{1/3}Co_{1/3}Mn_{1/3}O_2$ cathode material.

Acknowledgements

The authors acknowledge the partially financial support of the National Natural Science Foundation of China (Nos. 50236010, 20476055) and the program of New Century Excellent Talents in University of China (2004).

References

[1] K. Mizushima, P.C. Jones, P.J. Jones, P.J. Wiseman, J.B. Goodenough, Mater. Res. Bull. 17 (1980) 783.
[2] T. Ohzuku, A. Ueda, J. Electrochem. Soc. 141 (1994) 2972.
[3] Z.F. Ma, X.Q. Yang, X.Z. Liao, X. Sun, J. McBreen, Electrochem. Commun. 3 (2001) 425.
[4] Z.L. Gong, H.S. Liu, X.J. Guo, Z.R. Zhang, Y. Yang, J. Power Sources 136 (2004) 139.
[5] S.-T. Myung, S. Komaba, N. Kumagai, J. Electrochem. Soc. 148 (2001) A482.
[6] Z.F. Ma, X.Q. Yang, X. Sun, J. McBreen, J. New Mater. Electrochem. Syst. 4 (2001) 121.
[7] T. Ohzuku, Y. Makimura, Chem. Lett. 7 (2001) 642.
[8] Z. Lu, D.D. MacNeil, J.R. Dahn, Electrochem. Solid-State Lett. 4 (2001) A191.
[9] I. Belharouak, Y.-K. Sun, J. Liu, K. Amine, J. Power Sources 123 (2003) 247.
[10] Y.M. Todorov, K. Numata, Electrochim. Acta 50 (2004) 495.
[11] J. Choi, A. Manthiram, Electrochem. Solid-State Lett. 8 (2005) C102.
[12] G.-H. Kim, J.-H. Kim, S.-T. Myung, C.S. Yoon, Y.-K. Sun, J. Electrochem. Soc. 152 (2005) A1707.
[13] M.-H. Lee, Y.-J. Kang, S.-T. Myung, Y.-K. Sun, Electrochim. Acta 50 (2004) 939.
[14] T.H. Cho, S.M. Park, M. Yoshio, T. Hirai, Y. Hideshima, J. Power Sources 142 (2005) 306.
[15] A. Caballero, M. Cruz, L. Hernan, M. Melero, J. Morales, E.R. Castellon, J. Power Sources 150 (2005) 192.
[16] X.R. Ye, D.Z. Jia, J.Q. Yu, X.Q. Xin, Z. Xue, Adv. Mater. 11 (1999) 941.
[17] E.G. Gillan, R.B. Kaner, Chem. Mater. 8 (1996) 333.
[18] B.W. Lee, J. Power Sources 109 (2005) 220.
[19] K.S. Park, M.H. Cho, S.J. Jin, K.S. Nahm, Electrochem. Solid-State Lett. 7 (2004) A239.
[20] P.Y. Liao, J.G. Duh, S.R. Sheen, J. Electrochem. Soc. 152 (2005) A1695.
[21] Z. Wang, Y. Sun, L. Chen, X. Huang, J. Electrochem. Soc. 151 (2004) A1914.
[22] S.-H. Wu, C.W. Yang, J. Power Sources 146 (2005) 270.
[23] S.H. Park, C.S. Yoon, S.G. Kang, H.-S. Kim, S.-I. Moon, Y.-K. Sun, Electrochim. Acta 49 (2004) 557.
[24] J. Choi, A. Manthiram, Electrochem. Solid-State Lett. 8 (2005) C102.
[25] H. Cao, Y. Zhang, J. Zhang, B. Xia, Solid State Ionics 176 (2005) 1207.
[26] S. Gopukumar, K.Y. Chung, K.B. Kim, Electrochim. Acta 49 (2004) 803.
[27] C. Gan, X. Hu, H. Zhan, Y. Zhou, Solid State Ionics 176 (2005) 687.